Tribol Lett (2008) 32:1–11
DOI 10.1007/s11249-008-9353-y

ORIGINAL PAPER

Use of Eyring Equation to Explore the Frictional Responses of a $-CF_3$ and a $-CH_3$ Terminated Monolayers Self-Assembled on Silicon Substrate

K. Subhalakshmi · D. Devaprakasam · S. Math · S. K. Biswas

Received: 27 October 2007 / Accepted: 5 August 2008 / Published online: 27 August 2008

Abstract Lateral force microscopy is used to measure the frictional forces generated in sliding a silicon nitride tip on perflurooctyl trichlorosilane (FOTS) and octadecyltrichlorosilane (ODTS) monolayers self-assembled (SAM) on silicon wafer. The work is motivated by a need to rationalize the high friction of FOTS in comparison to that found for ODTS, inspite of the former having a low surface energy compared to that of the latter. Having first established that the tribology here is a thermally activated process, we use the Eyring equation to estimate the energetic barrier height to sliding motion, system activation energy, shear coordination and pressure activation volumes. For a molecular species when the velocity and temperature are unchanged in a sliding experiment and the activation energy remains unchanged the change in shear coordination with increasing normal load controls the friction coefficient. In comparing the performance of the two test molecules the friction coefficient of the FOTS is found to be three times greater than that of the ODTS; the corresponding difference in barrier height is about 10%. Our results indicate that when the two molecules are well ordered, the shear coordination modulates the frictional differential but it is the difference in their system activation energy, principally determined by electrostatic repulsion between the neighbouring molecules which is a dominant influence on their friction differential.

Keywords Fluorocarbons · Boundary lubrication friction · Friction mechanisms · Automotive industry

K. Subhalakshmi · D. Devaprakasam · S. Math · S. K. Biswas (✉)
Department of Mechanical Engineering, Indian Institute of Science, Bangalore 560012, India
e-mail: skbis@mecheng.iisc.ernet.in

1 Introduction

When surfaces are functionalized with self-assembled monolayers and slid against a rigid probe, a finite force of friction prevails at zero normal load and on increasing the normal load the friction force may increase linearly with or without slick-slip with normal load [1]. This model suggests that higher the adhesion, higher is the friction force. The friction of CF terminated monolayers is found to be greater [2–8] than that of CH terminated monolayers although the adhesion of the former is [9–11] less than or similar to that of the latter. As fluroalkyl and alkane are important tribological molecules, this anomaly has given rise to much debate. The debate has led to the exploration of other physical and mechanical parameters which could distinguish between their frictional performances; molecular order [6], hysterisis [12], size of terminal atoms [7], local packing environments [8], energetic barriers to molecular motion [7, 13, 14], molecular stiffness [11, 15] phase state [16], hydrophobicity [15, 17] and steric interaction [7]. Most of these parameters influence the barrier energy to molecular motion. McDermott et al. [14] discussed coefficient of friction in the context of the Eyring equation which gives a full fledged expression for this barrier in terms of shear activation volume (ϕ), the pressure activation volume (Ω) and activation energy of the system (Q). It is acknowledged that the Eyring equation provides a semiempirical but thermodynamically appropriate method for choosing molecular lubricant [14, 18, 19]. In this paper, we use lateral force microscopy (LFM) to estimate the constituent terms of the Eyring equation and the barrier energy for perflurooctyltrichlorosilane and octadecyltricholorosilane molecules self-assembled on silicon wafer.

2 Experimental

1H, 1H, 2H, 2H—perfluroalkyltriochlorosilane (FOTS) and octadecyltrichlorosilane (ODTS), of 99% purity (Sigma–Aldrich, USA) were self-assembled on silicon [100] substrate. The substrates were ultrasonically cleaned in 50:50 acetone–water solutions for 45 min and then uv cleaned (BIOFORCE–uv) for 1 h. The substrate was immediately transferred to freshly prepared 1 mM FOTS and ODTS solution. After 30 min of dipping, the samples were transferred to desicators, purged with ultra-pure nitrogen and maintained in an evacuated (10^{-3} mm of Hg) chamber, prior to being transferred to the chambers of the atomic force microscope.

The samples were characterized using grazing angle FTIR (Perkin-Elmer GX) to establish their ordered monolayer status. The instrument is equipped with a liquid nitrogen cooled mercury cadmium telluride (MCT) detector. Silicon wafer substrate is used as a reference for all IR using 1024 optimized scans at 4 cm^{-1} resolution using p-polarized beam. The sample and the detector are purged with nitrogen before starting experiments. A heating accessory (Harrick scientific corporation, NY, USA) is used to increase the temperature of the sample. The spectrum analysis is carried out using spectrum 3.02 version software (Perkin-Elmer, USA).

To check the polymerization of the FOTS SAM, we had [20] compared the IR spectra with those obtained for the molecules assembled from the gas phase. Close identity of the two spectra indicates that the FOTS monolayer assembled here is well packed with minimal lateral polymerization. Presence of strong (Si–O–Si) and silanol peaks as compared to their absence in the bulk ODTS [21] suggests that the present SAMs are not hydroxylated and minimally cross-polymerized. The observed sharpness of the room temperature methylene peaks suggests that the monolayers are well packed at room temperature. The FWHM value at room temperature was found to be 14 cm^{-1} [22].

Friction experiments were performed using a commercial atomic force microscope (AFM) (Explorer, Thermomicroscope, Vecco, USA). Measurements were performed using square pyramidal Si_3N_4 tips of a nominal 30 nm radius, mounted on gold coated triangular Si_3N_4 cantilevers of normal spring stiffness of 0.15 N/m. The experiments were performed in a normal load range of 0–60 nN and a sliding velocity range of 100–1,600 nm/s. Each experiment was done on a 100 × 100 nm^2 scan area in 500 × 500 points. We present here an estimate of the average of the data collected at all the points in a single experiment (100 × 100 nm^2 scan). We also show the standard deviation ($\pm\sigma$) of the data corresponding to each average as collected from a single experimental scan. We repeated each experiment (scan) five times. The variation in the average, experiment to experiment, was never more than 5% of the average shown in the data presented here. A heating stage was used to vary the substrate temperature in the 330–380 K range. All experiments were conducted in the ambient at 23 °C and 0% relative humidity in a sealed chamber and the chamber was purged with dry N_2 continuously during the experiments. We have recorded the humidity in the chamber by keeping a hygrometer (BARIGO, Germany) inside it.

2.1 AFM Cantilever Calibration

We used a straight forward finite element (FEM) based technique to estimate the torsional or lateral stiffness of the 'V'-shaped cantilever that is used here. This method does not require a 'multiple cantilever' (where one cantilever is of rectangular geometry) (Green et al. [23]), additional mass (Cleveland et al. [24]) or a well defined scanning geometry (wedge calibration method [25]). The normal sensor (NR) response (A/m) is recorded from the repulsive part of the force distance curve. Known the normal cantilever stiffness (N/m) from the manufacturer and the current geometry during an experiment we estimate the normal force.

Writing an angular response AR = NR × L, where L is the length of the cantilever, the twist angle ϕ is recorded as LRA/AR, where LRA is the twist current. Known the real geometry of the cantilever (from SEM images) and the material properties of the cantilever, the FEM (ABAQUS) is used to determine the torsional stiffness T/ϕ. The torque T is estimated for known ϕ.

For the present cantilever the manufacturer specifies the normal stiffness = 0.15 N/m. The FEM estimation gives $T/\phi = 1.6 \times 10^{-9}$ Nm/rad. The ratio of (T/ϕ)/Normal stiffness = 10^{-8} m^2/rad compares with those reported by Green et al. [23] who used the Sader method (2.2×10^{-8} m^2/rad) and that formulated by Cleveland et al. (2.3×10^{-8} m^2/rad) to calibrate 'V'-shaped cantilevers.

3 Model

Assuming the average time for single molecular barrier-hopping is given by Boltzman distribution in a process, where there are a regular series of barriers which are overcome repeatedly, the Eyring equation gives [18, 19, 26] the shear stress as

$$\tau = \frac{K_B T}{\phi} \ln\left(\frac{V}{V_0}\right) + \frac{Q + p\Omega}{\phi}$$

where stress limit is high ($\tau\phi/K_B T > 1$, in the present experiment $\tau\phi/K_B T \approx 10$).

The potential energy barrier which may account for the overall frictional work is given by

$$E = Q + p\Omega - \tau\phi \tag{1}$$

where p is the mean (normal) pressure acting on the pressure activation volume Ω of the junction and ϕ is the process coherence volume or the size of the molecular segment which moves collectively in the tangential direction acted upon by the shear stress [18, 19, 26, 27]. The Eyring equation thus provides a means to relate some properties of a monolayer such as Q and V_0 as well as some structural parameters such as stress (ϕ) and pressure (Ω) activation volumes of the assembly to the friction. Going back to the motivation for the present work we take the cue from Bouhacina et al. [28] and first, knowing that sliding friction is a thermally activated process, attempt to relate the difference between the barrier heights (E) of the two test molecules to their frictional difference and then study the structural parameters to understand the cause for this difference.

Briscoe and Evans [18] described an experimental method to obtain the potential energy barrier. They use Surface Force Apparatus (SFA) to measure contact area (A) and therefore the shear stress τ as functions of (1) p (keeping V and T as constants), (2) V (keeping p and T as constants) and (3) T (keeping p and V as constants) to yield the following equations,

$$\tau = \tau_0 + \alpha p; \quad \text{at constant } V \text{ and } T; \tag{2}$$

where,

$$\tau_0 = \frac{1}{\phi}\left(K_B T \ln\left(\frac{V}{V_o}\right) + Q\right) \tag{2a}$$

and,

$$\alpha = \frac{\Omega}{\phi} \tag{2b}$$

$$\tau = \tau_1 - \beta T; \quad \text{at constant } p \text{ and } V; \tag{3}$$

where,

$$\tau_1 = \frac{1}{\phi}(Q + p\Omega) \tag{3a}$$

and,

$$\beta = -\frac{K_B}{\phi}\ln\left(\frac{V}{V_0}\right) \tag{3b}$$

$$\tau = \tau_2 + \theta \ln V; \quad \text{at constant } p \text{ and } T; \tag{4}$$

where,

$$\tau_2 = \frac{1}{\phi}(Q + p\Omega - K_B T \ln V_0) \tag{4a}$$

and,

$$\theta = \frac{K_B T}{\phi} \tag{4b}$$

τ_0, τ_1, τ_2, α, β and θ are measured from the sliding friction experiments and we need to estimate the four unknowns Ω, ϕ, Q and V_0 to obtain E. The three sets of experiments should ideally yield mutually consistent values of these four unknowns.

In this work we take $V_0 = 100$ m/s as a constant. In the estimation of the other Eyring parameters such as β, we find β to change by an order when V_0 is varied over twelve orders in the 10^6–10^{-6} m/s range (ϕ and V are of the orders of 10^{-27} m^3 and 10^{-9} m/s, respectively). For the present experimental conditions variation of V_0 has thus only a very marginal effect on the barrier height E. Briscoe and Evans [18] and Bouhacina et al. [28] came to the same conclusion and the latter suggested the use of a value of 100 m/s [jump distance = lattice constant ($b = 1$ nm) $\times$ process frequency (10^{11} Hz)]. We have used the same value here.

We may now use equation sets 2 and 4 to find out the values of ϕ, α *and* Q. We use Eq. 4b to calculate ϕ knowing the value of θ and then calculate Ω using Eq. 2b from a known value of α. We find out the activation energy (Q) using Eq. 4a. Substituting ϕ, Ω and Q in Eq. 1 the potential energy barrier, E, is estimated.

4 Results and Discussion

Figure 1 shows the shear stress (τ) variation of the two test molecules (ODTS and FOTS) as a function of the mean normal pressure (p). An average tangential force (F) is estimated at each normal load (N) by finding the half-width (average deviation from the mean) of the lateral force loop recorded in the forward and reverse scans in the LFM. The JKR model [29] is used to calculate the contact area (A) and obtain the shear stress τ (F/A) and the mean normal pressure (N/A). The material properties used in calculating the contact area are; surface energies, $\gamma_{\text{ODTS}} = 22.5$ mJ/m^2 [30], $\gamma_{\text{FOTS}} = 12.5$ mJ/m^2 [30] and Young's modulus of both the molecules = 1 GPa [15]. We give below our justification for estimating the shear stress from the friction force by using the JKR contact area formulation.

There has been much debate regarding the physics and mechanics of the empirical Amontons law which expresses the friction force as a linear function of the normal load. Brukman et al. [9] suggest that the functionality or the power of the normal load in this function depends on the nature of the contact. If the asperity or the scriber ploughs into the monolayer the area of contact 'A' is linearly proportional to the normal load N and for a ploughing shear stress τ_p independent of penetration, $F = \tau_p A = \text{const} \times N$. This type of contact therefore recovers the Amontons Law. If the contact is however a sliding one the co-efficient of friction may be expressed as, $\mu = (\tau_0/p) + \alpha$, for $\tau = \tau_0 + \alpha$ p, where α is the slope of the shear stress–pressure graph and τ_0 is the intercept. He et al. [31] and Brukman et al. [9] show that if $(\tau_0/p) \approx \alpha$, the friction force F may

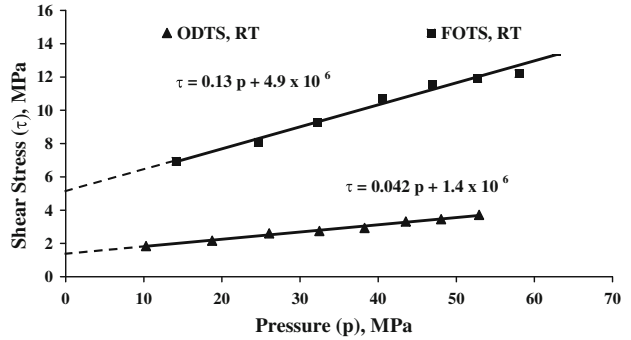

Fig. 1 Shear stress vs. normal pressure for FOTS and ODTS self-assembled on Si substrate at room temperature, velocity = 400 nm/s

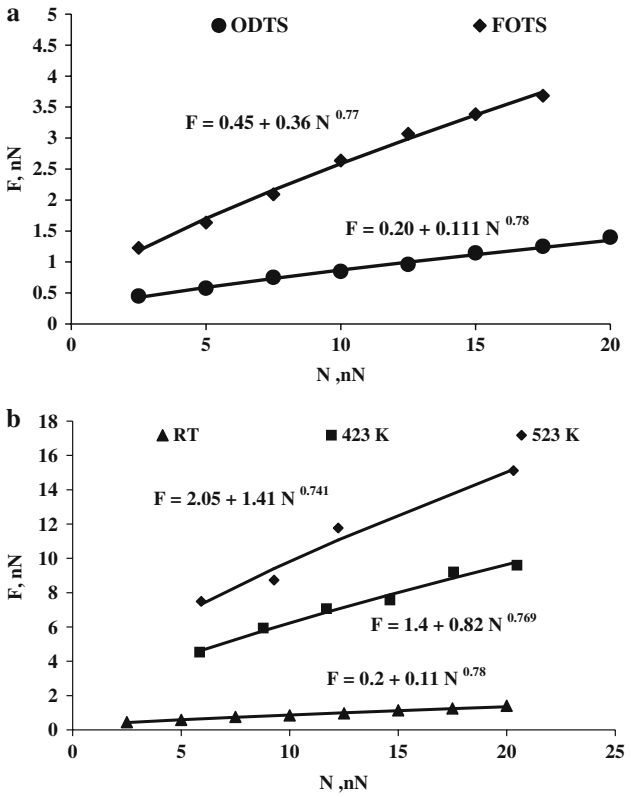

Fig. 2 (**a**) Friction force vs. normal load, for FOTS and ODTS self-assembled on Si substrate at room temperature. Velocity = 400 nm/s. (**b**) Friction force vs. normal load, ODTS self-assembled on Si substrate, heat-treated to different peak temperatures ◆ 523 K, ■ 423 K, ▲ 296 K (ambient temperature), velocity = 400 nm/s

be related non-linearly to load, while if $(\tau_0/p) << \alpha$, Amontons law is conserved. In the present case, $(\tau_0/p_{av}) \approx 0.16$ for FOTS and ≈ 0.046 for ODTS, the corresponding values of α are 0.13 and 0.042 (Fig. 1). The *F–N* non-linearity that we observe, as shown in Fig. 2a, demonstrates, as per the mechanism suggested by Brukman et al. [9] that the experiment was conducted under sliding (and not under ploughing) condition where the static ($N = 0$) shear stress plays an important role in determining the frictional response. The non-linearity of *F–N* curves is also observed for ODTS heat-treated at different peak temperatures as shown in Fig. 2b.

The measured friction force bears a non-linear relationship with the normal load as

$$F = A_0 + B_0 N^n$$

where, for FOTS, $n = 0.77, A_0 = 0.45 \times 10^{-9}, B_0 = 0.0030$; for ODTS, $n = 0.78, A_0 = 0.\,20 \times 10^{-9}, B_0 = 0.0012$.

Considering the non-zero intercept at $N = 0$ and $n < 1$, we believe the junction is adhesive. The JKR [29] contact areas for the present experimental configurations, known the surface energies, γ, are

$$\text{FOTS} - A = \left(1.4 \times 10^{-16} + 7.25 \times 10^{-11} N^{0.72}\right), \text{m}^2$$

$$\text{ODTS} - A = \left(2.09 \times 10^{-16} + 1.55 \times 10^{-11} N^{0.77}\right), \text{m}^2$$

The exponents of N for the friction force and the JKR areas being very similar we estimate the contact area A using the JKR formulation and estimate the shear stress as $\tau = \frac{F}{\pi}\left[\frac{6\pi\gamma R^2}{K} + \frac{NR}{K} + \sqrt{\frac{12\pi\gamma R^3 N}{K^2} + \left(\frac{6\pi\gamma R^2}{K}\right)^2}\right]^{-2/3}$, where R is the tip radius and $K = 4/3 \times E^*$ where E^* is the reduced Young's modulus of the tip.

The estimated contact areas are given in Table 1. The $\tau - p$ characteristics are linear and the slope α (Eq. 1) of the FOTS characteristics (0.13) is significantly greater than that of the ODTS characteristics (0.042). These values compare well with those reported by others [2, 7, 11, 13, 15, 32] for $-CF_3$, $-CH_3$ terminated self-assembled monolayers.

4.1 Thermally Activated Process

Figure 3 shows that the friction–velocity relationship is logarithmic for both the test molecules at room temperature at two different normal loads. The friction recordings (not shown) also exhibited pronounced stick–slip behaviour. A logarithmic friction–velocity relationship corresponds [26] to a discontinuous sliding process. For a given set of molecular assembly, such discontinuities are observed in appropriate velocity ranges. They are caused by activation barriers which are repeatedly overcome during the sliding

Table 1 Contact area at different experimental normal loads, using the JKR model for FOTS and ODTS molecules

ODTS		FOTS	
Load (nN)	Area ($\times 10^{-16}$ m^2)	Load (nN)	Area ($\times 10^{-16}$ m^2)
15	3.42	15	2.84
46.5	5.22	40	4.33
56	5.67	42.8	4.47

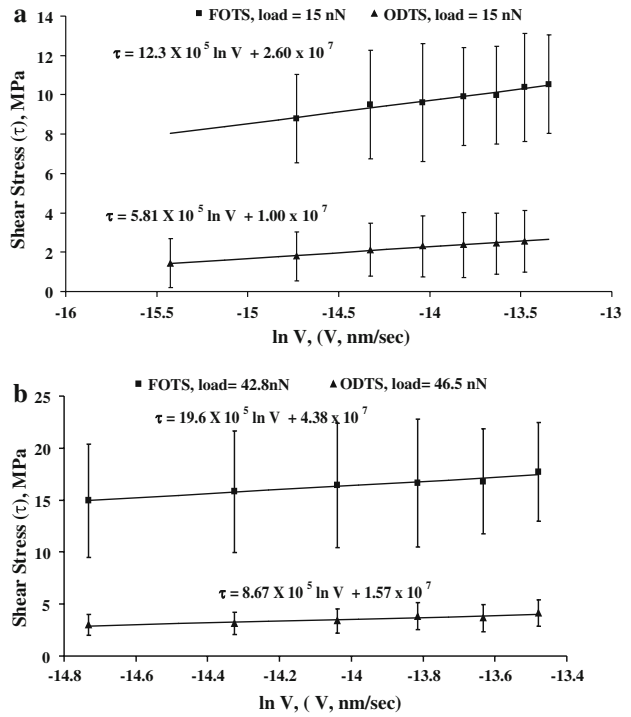

Fig. 3 (**a**) Shear stress vs. sliding velocity V, for FOTS and ODTS self-assembled on Si substrate at room temperature. Load = 15 nN. The error bars are $\pm\sigma$. (**b**). Shear stress vs. sliding velocity, V for FOTS and ODTS self assembled on Si substrate at room temperature. Load = 40–50 nN. The error bars are $\pm\sigma$

process. The process is thermally activated and exhibits a declining monotonic trend with temperature [18] above a critical temperature [33].

There is indeed another (apart from the Eyring equation) approach to analyse thermally activated processes. This uses the experimental stick-slip data. Gnecco et al. [34] demonstrated this using atomic level stick-slip data obtained from a lateral force microscope experiment on NaCl crystal. The stick-slip is a direct consequence of the probabilistic nature of the jump out of the Tomlinson potential wells in a non-zero temperature thermally activated process. The probabilistic function was established by Sang et al. [35] and Schirmeisen et al. [36] who demonstrated the validity of the function for molecular creep and showed that the jump becomes probable over wider ranges of lateral force as the temperature is increased. The latter implies that the lateral force to cause slip decreases with increasing temperature. Our present experimental data exhibits these (stick-slip, positive logarithmic force–velocity and negative force–temperature relations) characteristics of a thermally activated process, but we pursue the Eyring equation to analyse our experimental data because of the inherent ability of the Eyring model to distinguish the structural (shear coordination, pressure volume, repulsive activation energy) components of the barrier height. We do

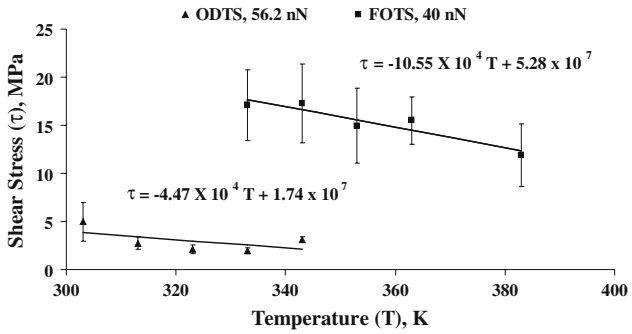

Fig. 4 Shear stress vs. temperature for FOTS and ODTS self assembled on Si substrate. Velocity = 400 nm/s. The error bars are $\pm\sigma$

a final validation of the model using the stress–temperature data.

The use of $V_0 = 100$ m/s in the present analysis allows to use the $[\text{shear stress–temperature}]_{p,V}$ data (Fig. 4) as an independent validatory test of the Eyring parameters derived using the $[\text{shear stress–velocity}]_{p,T}$ experimental data. Known the value of ϕ from Eq. 4b, we estimate β (Eq. 3b), for a given p and V. For FOTS; $\beta_{\text{Eyring}} = 12 \times 10^4$ N/m^2/K, $\beta_{\text{Expt}} = 10.55 \times 10^4$ N/m^2/K. For ODTS; $\beta_{\text{Eyring}} = 5.6 \times 10^4$ N/m^2/K, $\beta_{\text{Expt}} = 4.47 \times 10^4$ N/m^2/K, ($N = 40$ nN for FOTS and 56 nN for ODTS, $V = 400$ nm/s). Given the scatter of the experimental data, we believe the Eyring parameters predict well the shear stress–temperature slope. Given this and the fact that the estimated process activation energy (Q) arising out of intermolecular repulsion (45–50 kJ/mol) accord well with those reported by others [18, 26, 28, 37] for a variety of lubricant systems, give confidence in the use of the Eyring model for analysing and understanding the mechanisms of dissipation involved in sliding of organic monolayers.

Figures 3 and 4 thus legitimize the use of the Eyring equation (Eq. 1) as rendered by Briscoe and Evans [18]. Table 2 gives the values of the various Eyring parameters estimated from the experimental friction data. The α value obtained from experiment 1 is used in conjunction with other experimental data to provide the estimates shown in the Table 2.

Table 2 shows that the barrier energy height increases with normal load and is higher for the FOTS molecules than for the ODTS molecules. Barrier energy to molecular motion would thus appear to reflect, at least qualitatively, the frictional resistance and the approach provides a means to explore properties of the film such as the activation energy Q and structural parameters ϕ and Ω, which have bearings on resistance to tangential molecular motion.

Briscoe and Evans [18] had used a SFA to analyse their friction data using the Eyring equation. We justify the use of the same approach to analyse data, but using the AFM, as follows. The area calculated using JKR model depends

Table 2 Eyring equation parameters for FOTS and ODTS

SAM	Experiment 1a		Experiment 1b	
	$T = 295$ K, $P = 42.8$–46.5 nN		$T = 295$ K, $P = 15$ nN	
	FOTS (1) $P = 42.8$ nN	ODTS (2) $P = 46.5$ nN	FOTS (3) $P = 15$ nN	ODTS (4) $P = 15$ nN
1. α	0.13	0.042	0.13	0.042
2. ϕ, nm^3	2.08	4.69	3.31	7.00
3. ϕ/A, nm	0.0046	0.0089	0.012	0.021
4. Ω, nm^3	0.2704	0.1972	0.4302	0.2940
5. $\tau\phi$, kJ/mol	21.8219	14.5395	23.7607	13.4915
6. $p\Omega$, kJ/mol	15.5899	10.5824	13.9722	7.7727
7. $(p\Omega - \tau\phi)$, kJ/mol	−6.2320	−3.9571	−9.7885	−5.7188
8. Q, kJ/mol	50.75	45.05	50.11	44.27
9. E, kJ/mol	44.51	41.09	40.02	38.52

on the surface energy, radius of the tip and reduced Young's modulus. The radius of the tip is the same for all the experiments and the Young's modulus of both SAMs are assumed 1 GPa [15]. So the error in calculated area is solely dependant on the error in the measurement of surface energy of the monolayers. The error in surface energy is 5.28% for FOTS and 2.43% for ODTS [30], and the corresponding errors in calculated area are 0.1435% and 0.08611% for FOTS and ODTS, respectively, because the area in JKR formulation varies with two-third power of the surface energy. Unlike in a SFA experiment where one has access to absolute values of the contact area, in an AFM experiment the estimate of the contact area may be questionable in terms of its absoluteness (for example, the exact value of the tip geometry is unknown). However given an assumed radius, the error in area estimation is minimal. In this paper we are concerned with the relative values of the Eyring parameters, between two molecules. We believe that given the certainty in area estimation, for an assumed tip radius, the relative magnitudes are correct and the inferences drawn using these relative magnitudes may be considered to be valid.

The distinction between these two molecules in their Q value (10%) is quite substantial and it is two orders more than the error coming in some of the Eyring parameters due to error in estimated area.

4.2 Heat-treated Disordered ODTS Monolayers

Before proceeding to rationalize the friction differential between FOTS and ODTS SAMs, we first examine some existing notions of friction expounded using the Eyring equation. We do this by examining the Eyring parameters ϕ and Ω deconvoluted from frictional experiments done on heat-treated ODTS SAMs. Overney [19] and He et al. [26] had postulated that when the film thickness of slid *n*-hexadecane is of the order of a few nanometers, the molecules shear coordinate to align in the sliding direction and the friction is consequently low. Mcdermott et al. [14] working with alkanethiols of different chain lengths make a similar observation. Long chain molecules held together by strong interchain Van der Waal forces are well ordered. In this case, it is possible to accommodate large shear coordination (ϕ) with only a limited change (Ω) in local volume. The ratio $\alpha = \Omega/\phi$ is small and the friction is low, α controls the slope of the friction shear stress with contact pressure. When the structure is disordered with chain entanglements and gauche defects, as for example in a thick film of *n*-hexadecane or a short chain chemiadsorbed alkanethiol, large change in local volume is registered to reorganize the molecules to implement even a small shear (high Ω, low ϕ). The tendency in this case is for the molecules to respond to traction as individuals and not as a coordinated collective body. The value of α (Ω/ϕ) is high and the friction is high.

We first explore the "structural reorganization" argument of He et al. 26] and McDermott [14] by carrying out frictional studies on ODTS molecules which have been cyclically heated to make them more disordered. Self-assembled on silicon substrates, the molecules were heated to different peak temperatures and cooled down to room temperature. Vibrational spectra of the SAM after such heat treatment were taken with FTIR. Figure 5 shows that conformational disorder increases with increasing peak heat treatment temperature. Figure 6 shows the friction coefficient to also increase significantly with increasing peak temperature. The corresponding Eyring parameters are shown in Table 3. Table 3 has been deconvoluted using the data presented in Fig. 6. The table shows that when the SAM is heat-treated, there is an increase in local volume change (Ω), a reduction in shear coordination (ϕ), an increase in activation energy (Q) and an overall increase

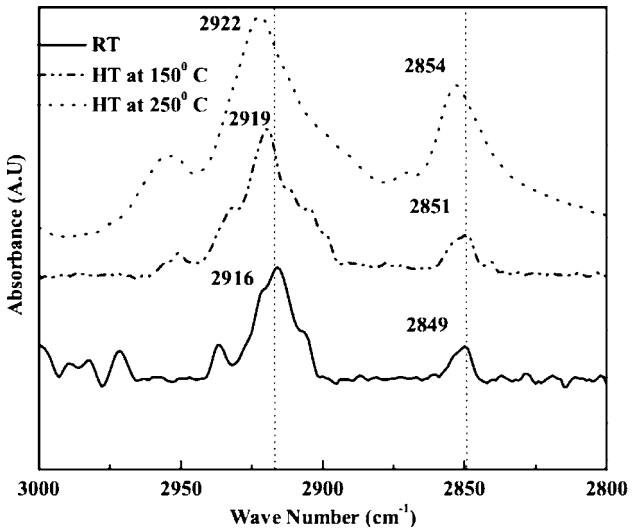

Fig. 5 FTIR spectra of ODTS heat–treated to different peak temperatures; RT (296 K)

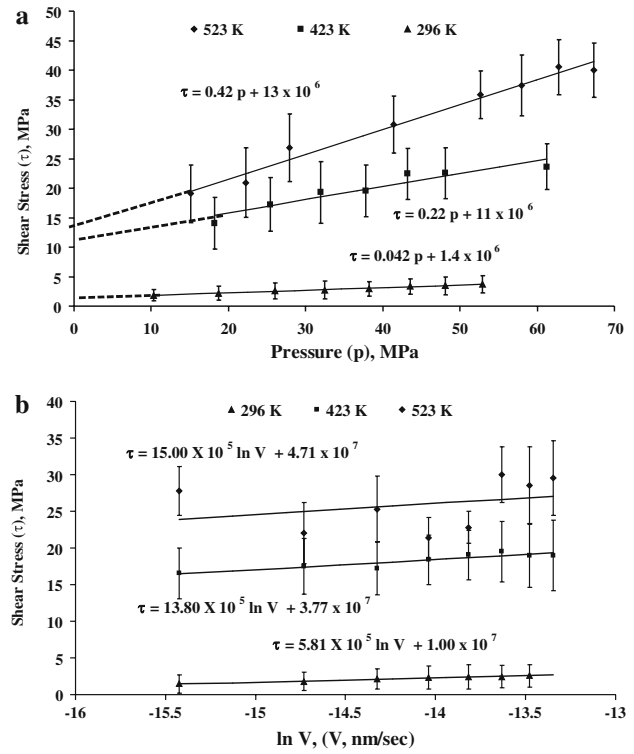

Fig. 6 (**a**) Shear stress vs normal pressure, ODTS self assembled on Si substrate, heat-treated to different peak temperatures ◆ 523 K, ■ 423 K, ▲ 296 K (Ambient temperature), velocity = 400 nm/s. The error bars are $\pm\sigma$. (**b**) Shear stress vs. sliding velocity, V, ODTS self assembled on Si substrate, heat-treated to different peak temperatures ◆ 523 K, ■ 423 K, ▲ 296 K (ambient temperature). Load = 15 nN. The error bars are $\pm\sigma$

in barrier height (E). The Eyring parametric data in conjunction with the FTIR results validate the observation of He et al. [26] that shear coordination and coherence length

Table 3 Eyring equation parameters for heat-treated ODTS samples

Heat treatment temperature at load = 15 nN	*RT*	423 K	523 K
α	0.042	0.22	0.42
ϕ, nm^3	7.00	2.95	2.71
ϕ/A, nm	0.021	0.0076	0.0059
Ω, nm^3	0.2940	0.6490	1.1399
$\tau\phi$, kJ/mol	13.4915	34.5817	43.7776
$p\Omega$, kJ/mol	7.7727	15.0473	22.5284
$(p\Omega - \tau\phi)$, kJ/mol	−5.7188	−19.5344	−21.2492
Q, kJ/mol	44.27	63.12	65.83
E, kJ/mol	38.52	43.59	44.58

decreases as the molecular structure becomes more disordered. Further, it supports the contention of McDermott et al. [14] that when a molecular structure is made more disordered greater local volume change is necessary to implement a unit shear coordination. This corresponds to an increase in coefficient of friction.

The MD simulation work of Harrison and coworkers have provided a benchmark for studying the effect of molecular disorder on friction. In flat plate commensurate sliding [38] of well packed organic monolayers comprising even number of carbon atoms they show that molecules maintain all-*trans* configuration under load, the adjacent molecules become 'locked' in this configuration to move in a synchronized manner during sliding [39]. This is an ideal low friction system. If non-coherent molecular movements are made possible by sliding on a monolayer of reduced packing density [40], sliding on molecules with odd number of carbon atoms [38] and sliding on mixed monolayers [41], the energy dissipation modes are enhanced over the ideal system. Incoherent and out of plane molecular movements dissipate energy, additional to that dissipated by molecular vibration. The authors argue that these disable the molecules from ploughing back substantial energy on their 'spring back', to the substrate, additional modes to neutralize some of the elastic work done on the molecules in their forward journey. When the flat slider is replaced by an 'AFM' type of tip, substantial number of gauche defects are also generated at the terminal and backbonal levels, and this further enhances the modes of energy dissipation and increases the friction force [42–45]. The studies quoted above lays the foundation for a model which states that increasing molecular disorder disrupts synchronous or coherent movement of molecules in the sliding direction and the consequence is an enhancement of friction. One could now argue in the context of the Eyring model that when the molecules move in a synchronous manner and the behaviour is coherent, only a small volume change (Ω) is

Table 4 Peak frequency and FWHM at different heat-treated temperatures

	Peak frequency (cm^{-1}), d^- stretch	Peak frequency (cm^{-1}), d^+ stretch	FWHM (cm^{-1}), d^- stretch
RT	2922.08	2853.78	14.93
423 K	2919.41	2851.11	17.89
523 K	2916.30	2849.33	22.94

necessary to institute shear and this reduces the energy barrier to molecular hopping in a sliding motion.

We have studied [21, 22] the effect of heat treating an ODTS monolayer on the vibrational spectra of the symmetric and anti-symmetric methylene and methyl (r^-) stretches. On cyclic heating to different peak temperatures the residual integrated intensity, peak frequency and FWHM increase with peak temperature. For example, we found the residual packing density to decrease as the corresponding FWHM increased from 15 to 18 cm^{-1}, in response to an increase in peak temperature from 23 to 150 °C. A steady increase in residual peak frequency, that we observe with peak heat-treatment temperature, indicates a general increase in disorder. The increase that we observe in integral intensity and untilting with peak temperature indicates an increase in gauche defect population [21, 46, 47]. Comparing the spectra of the methylene (d^-) and methyl (r^-) we further deduce that while gauche defects accumulate at the terminal end till about 90 °C (peak temperature), at higher peak temperatures they penetrate significantly into the backbone. Our results indicate that when the molecules are cooled back to room temperature the backbonal gauche defects remain trapped even when the terminal groups anneal.

Thus the ODTS monolayer, well packed at room temperature, looses its packing density as well as become more disordered and full of rotational defects when it is heat-treated (Table 4). The MD simulation studies quoted above would thus suggest that shear coordination and synchronization in sliding of a monolayer become more difficult when the monolayer is in a heat-treated state.

4.3 Effect of Normal Load on Friction

Here we comment on the rationale for the increasing friction force with normal load for both the test molecules.

Equation 1 may be rewritten as

$$\begin{aligned} E &= Q + (p\Omega - \tau\phi) \\ &= Q + \{p\alpha\phi - (\tau_0 + \alpha p)\phi\} \\ &= Q - \tau_0\phi \end{aligned} \tag{5}$$

Differentiating Eq. 5 with respect to the normal load; N, if Q and τ_0 are constants;

$$\frac{dE}{dN} = -\tau_0 \frac{d\phi}{dN}$$

If $\frac{d\phi}{dN}$ is negative, $\frac{dE}{dN}$ is positive and the barrier height increases with normal load.

For a given molecule Table 2 shows that Q changes only marginally with increasing load and τ_0 is of course a constant. The shear coordination volume, ϕ (and the coherence length) is thus the only parameter which accounts for the change in barrier height with changing load.

Table 2 shows that for both the test molecules, ϕ and ϕ/A decreases substantially with increasing normal load. The resultant is an increase in barrier energy height. We also note that while the coefficient of friction remains unchanged with increasing load, the friction force increases by 3.25 and 1.05 nN for the FOTS and ODTS molecules, respectively, when the normal load is increased from 15 to above 40 nN.

Increase in the gauche defect population (especially in an AFM experiment) at the terminal and backbonal levels [36, 41, 42, 45] and molecular tilting, due to an increase in normal load bring about conformational changes which undermine the more coherent and synchronous behaviour (low ϕ) observed at the lower loads. Avenues of energy dissipation are consequently increased and there is a rise in the friction force. We have shown later (Sect. 4.2) that coherent behaviour is severely undermined when there is apriori disorder in the SAM.

4.4 Ordered FOTS and ODTS Monolayers

In comparing the performance of ODTS and FOTS, Table 2 shows that shear coordination ϕ and coherence length of FOTS are significantly smaller than that of ODTS. Further, the local volume change necessary to implement shear is greater for the FOTS than for the ODTS yielding a higher coefficient of friction for FOTS than for the ODTS. These observations are very similar to those made (Sect. 4.3) when a molecular structure is made more disordered. FOTS and ODTS in their self-assembled state are however well ordered [15, 20] and have similar packing densities [48]. So why does ODTS respond with greater shear coordination to sliding traction and a corresponding smaller change in local volume than what is done by the FOTS? We do not have the final answer to this question but do believe at this stage that the reason for this difference lies in the fact that FOTS molecules are stiffer than the ODTS molecules. In studying the friction of a mixed monolayer of fluorocarbon and hydrocarbon Meyer et al. [49] found the hydrocarbon island to shear away easily while the fluorocarbon remained intact under the same traction. The friction recorded for the hydrocarbon islands was four times less than that of the fluorocarbons. Nanoindentation tests of the phases also

showed large deformation of the hydrocarbon but a great resistance to rupture and no deformation for the fluorocarbon. The large shear plasticity observed for hydrocarbons is attributed to the presence of structural defects such as holes and grooves. The significantly higher stiffness of the fluorocarbon molecules than that of the hydrogenated molecules have been demonstrated by a number of authors [49–51]. In a previous paper [20] we have attributed the high stiffness of fluroalkyls to its helical structure.

Shear coordination does not necessary mean an overall decrease in friction as we observe by comparing the structural energy factor $(-\tau\phi + p\Omega)$ for the two test molecules. Table 2 shows that although for FOTS, ϕ is low and Ω/ϕ is high compared to those of the ODTS, this structural energy factor which is subtracted from the activation energy to give the barrier height is greater for FOTS than for ODTS. If both the molecules had the same activation energy, FOTS would have a lower barrier height and a lower friction compared to that of the ODTS. This is clearly not so because the activation energies of the two molecules are significantly different and this difference supercedes the difference in barrier energy modulation brought about by their different abilities to shear coordinate. The situation is portrayed schematically in Fig. 7. Intermolecular repulsive energy thus plays an important role in conjunction with the ability of the molecules to shear coordinate in determining frictional resistance of the assembly to sliding motion.

Q is the repulsive energy between the adjacent molecules. The repulsive energy of FOTS is 5–6 kJ/mol higher than that of the ODTS. This is because of the large electronegativity of the $-CF_3$ group [52] which yields high electrostatic repulsion. The large radius of the fluorine molecules does give rise to substantial attractive Vander Waal forces, but the attractive forces (vary as the inverse of seventh power of separation, i.e., $1/r^7$, r being the distance of separation between interaction pairs) are smaller than the electrostatic repulsive forces (vary as the inverse of fourth power of separation, i.e., $1/r^4$) [52]. The Van der Waal force between fluorinated terminal groups is of the order of 0.0004 nN, one order smaller than the electrostatic force. The repulsive force between two similar terminal groups in free space can be obtained by differentiating the repulsive energy ($w(r) = \frac{-2u^2}{4\pi\varepsilon_0 r^3}$ [53], w, u, ε_0 and r being the interaction energy, dipole moment of the group, dielectric permittivity of free space (8.854×10^{-12} C^2 J^{-1} m^{-1} [53]) and distance between the groups, respectively) with respect to the distance parameter r. The dipole moment of $-CF_3$ in an aliphatic compound is 2.3 D [52] (1 D (Debye) = 3.336×10^{-30} C m), which is much higher than that of a hydrogenated group ($C-{}^{+}CH_3$ has a group moment of 0.4 D [53]). Hence, taking the separation between the terminal fluorine and hydrogen atoms in neighbouring chains to be 1.0 and 0.87 nm, respectively [54], the repulsion force between the neighbouring fluorine atoms is 0.0032 nN compared to 0.00016 nN for the hydrogenated group. This repulsion between terminal groups of neighbouring molecules in a SAM influences the repulsion between the chains and as per the reasoning given above is the dominant reason for the high barrier height observed for the FOTS in comparison with that for the ODTS. The high level of intermolecular forces between the neighbouring molecules in FOTS may also be responsible for its high torsional and translational rigidity which would tend to discourage shear coordination.

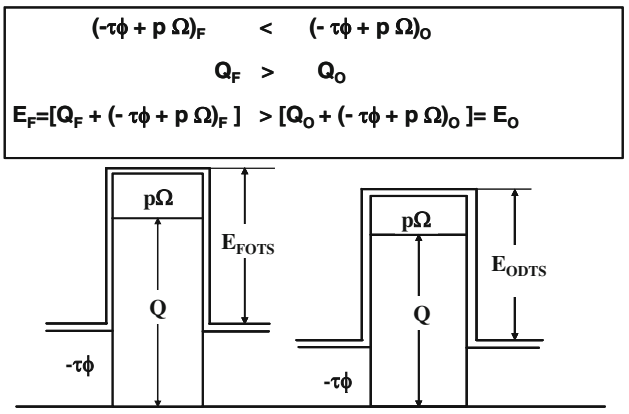

Fig. 7 Schematic of the construction of the intermolecular potential energy barrier to molecular motion, drawn roughly to scale for the two test molecules FOTS and ODTS

5 Conclusions

To address the issue of high friction of $-CF_3$ terminated monolayers in comparison with that of a $-CH_3$ terminated monolayers, both self-assembled on silicon, we measured lateral forces in an AFM. The experiments were performed by varying normal load, sliding velocity and temperature, one at a time and the data analysed within the framework of Eyring equations, as the process was found to be thermally activated. For perfluorooctyltrichlorosilane the shear coordination was found to be much less and the change in local volume to accommodate unit shear was found to be greater than those for octadecyltrichlorosilane. These differences in structural responses between these molecules were found to modulate the differences between their barrier energies to molecular motion in sliding. The dominant factor which differentiates their barrier energies and therefore friction was however found to be the intermolecular electrostatic repulsion energy. The latter is primarily determined by the size of the terminal group and the separation distance between adjacent molecules. The possibility of such a rationale has been discussed in a previous work [7].

Acknowledgements The authors are grateful to the support provided by Centre for High Technology, Ministry of Petroleum,Government of India to carry this work. We are grateful to Ms. Geetha and Ms. Savitha for assisting in the AFM experiments.

References

1. Gao, J., Luedtke, W.D., Gourden, D., Ruths, M., Israelachvili, J.N., Landman, U.: Frictional forces and Amontons' law: from the molecular to the macroscopic scale. J. Phys. Chem. B **108**(11), 3410–3425 (2004). doi:10.1021/jp036362l
2. Sung, I.-H., Yang, J.-C., Kim, D.-E., Shin, B.-S.: Micro/nano-tribological characteristics of self-assembled monolayer and its application in nano-structure fabrication. Wear **255**, 808–818 (2003). doi:10.1016/S0043-1648(03)00058-9
3. Takahara, A., Kojio, K., Kajiyama, T.: Effect of aggregation state on nanotribological behaviors of organosilane monolayers. Ultramicroscopy **91**, 203–213 (2002). doi:10.1016/S0304-3991(02)00100-6
4. Kojio, K., Takahara, A., Kajiyama, T.: Molecular aggregation state and molecular motion of organosilane monolayers prepared at the air/water interface. Langmuir **16**(24), 9314–9320 (1997). doi:10.1021/la0004303
5. Kim, H.I., Graupe, M., Oloba, O., Koini, T., Imaduddin, S., Lee, T.R., et al.: Molecularly specific studies of the frictional properties of monolayer films: a symmetric comparison of CF_3–$(CH_3)_2$ CH–, and CH_3 terminated films. Langmuir **15**, 3179–3185 (1999). doi:10.1021/la981497h
6. Schonherr, H., Vansco, G.: Tribological properties of self-assembled monolayers of flurocarbon and hydrocarbon thiols and disulfides on Au (111) studied by scanning force microscopy. Mater. Sci. Eng. C **8–9**, 243–249 (1999). doi:10.1016/S0928-4931(99)00041-7
7. Kim, H.I., Koini, T., Lee, T.R., Perry, S.S.: Systematic studies of the frictional properties of fluorinated monolayers with atomic force microscopy: comparison of CF_3- and CH_3-terminated films. Langmuir **13**, 7192–7196 (1997). doi:10.1021/la970539j
8. Li, S., Cao, P., Colorado, R., Yan Jr., X., Wenzl, I., Shamakova, O.E., et al.: Local packing environment strongly influences the frictional properties of mixed CH_3- and CF_3-terminated Alkanethiol SAMs on Au (111). Langmuir **21**, 933–936 (2005). doi:10.1021/la0488607
9. Brukman, M.J., Marco, G.O., Dunbar, T.D., Boardman, L.D., Carpick, R.W.: Nanotribological properties of alkanephosphonic acid self-assembled monolayers on aluminium oxide: effects of fluorination and substrate crystallinity. Langmuir **22**, 3988–3998 (2006). doi:10.1021/la052847k
10. Lio, A., Charych, D.H., Salmeron, M.: Comparative atomic force microscopy study of the chain length dependence of frictional properties of alkanethiols on gold and alkylsilanes on mica. J. Phys. Chem. B **101**, 3800–3805 (1997). doi:10.1021/jp963918e
11. Graupe, M., Koini, T., Kim, H.I., Garg, N., Miura, Y.F., Takenga, M., et al.: Self-assembled monolayers of CF_3-terminated alkanethiols on gold. Col. Surf. A. Phys. Eng. Aspects **154**, 239–244 (1999). doi:10.1016/S0927-7757(98)00902-9
12. Kiely, J.D., Houston, J.E., Mulder, J.A., Hsung, R.P., Zhu, X.Y.: Adhesion, deformation and friction for self assembled monolayers on Au and Si surfaces. Tribol. Lett. **7**, 103–107 (1999). doi:10.1023/A:1019109117742
13. Kim, H.I., Koini, T., Lee, T.R., Perry, S.S.: Molecular contributions to the frictional properties of fluorinated self-assembled monolayers. Tribol. Lett. **4**, 137–140 (1998). doi:10.1023/A:1019119608713
14. McDermott, M.T., Green, J.-B.D., Porter, M.D.: Scanning force microoscopic explanation of the lubrication capabilities of n-alkanethiolate monolayers chemisorbed at gold: structural basis of microscopic friction and wear. Langmuir **13**, 2504–2510 (1997). doi:10.1021/la962099m
15. Khatri, O.P., Devaprakasam, D., Biswas, S.K.: Frictional responses of Octadecyltrichlorosilane (OTS) and 1 H, 1H, 2H, 2H–Perflurooctyltrichlorosilane (FOTS) monolayers self-assembled on aluminium over six orders of contact length scale. Tribol. Lett. **20**(3–4), 235–246 (2005). doi:10.1007/s11249-005-8551-0
16. Lee, D.H., Oh, T., Cho, K.: Combined effect of chain length and phase state on adhesion/friction behaviour of self-assembled monolayers. J. Phys. Chem. B **109**, 11301–11306 (2005). doi:10.1021/jp051232t
17. Lieu, Y., Evans, D.F., Song, Q., Grainger, D.W.: Structure and frictional properties of self-assembled surfactant monolayers. Langmuir **12**, 1235–1244 (1996). doi:10.1021/la950504o
18. Briscoe, B.J., Evans, D.C.B.: The shear properties of Langmuir-Blodgett layers. Proc. R. Soc. Lond. A Math. Phys. Sci. **380**, 389–407 (1982). doi:10.1098/rspa.1982.0048
19. Overney, R.M., Tyndall, G., Frommer, J.: Kinetics and energetics in nanolubrication. In: Bhushan, B. (ed.) Nanotechnology Handbook, pp. 1–16, Chapter 29 . Springer, Heidelberg (2004)
20. Devaprakasam, D., Sampath, S., Biswas, S.K.: Thermal stability of perfluoroalkyl silane self-assembled on a polycrystalline aluminum surface. Langmuir **20**, 1329–1334 (2004). doi:10.1021/la0359676
21. Khatri, O.P., Biswas, S.K.: Thermal stability of octadecyltrichlorosilane self-assembled on a polycrystalline aluminium surface. Surf. Sci. **572**, 228–238 (2004). doi:10.1016/j.susc.2004.08.037
22. Khatri, O.P., Bain, C.D., Biswas, S.K.: Effects of chain length and heat treatment on the nanotribology of alkylsilane monolayers self-assembled on a rough aluminium surface. J. Phys. Chem. B **109**, 23405–23414 (2005). doi:10.1021/jp054074e
23. Green, C.P., Lioe, H., Cleveland, J.P., Proksch, R., Mulvaney, P., Sader, J.E.: Normal and torsional spring constants of atomic force microscope cantilevers. Rev. Sci. Instrum. **75**(6), 1988–1996 (2004). doi:10.1063/1.1753100
24. Cleveland, J.P., Manne, S., Bocek, D., Hansma, P.K.: A nondestructive method for determining the spring constant of cantilevers for scanning force microscopy. Rev. Sci. Instrum. **64**(2), 403–405 (1993). doi:10.1063/1.1144209
25. Ogletree, D.F., Carpick, R.W., Salmeron, M.: Calibration of frictional forces in atomic force microscopy. Rev. Sci. Instrum. **67**(9), 3298–3306 (1996). doi:10.1063/1.1147411
26. He, M., Blum, A.S., Overney, G., Overney, R.M.: Effect of interfacial liquid structuring on the coherence length in nanolubrication. Phys. Rev. Lett. **88**(15), 154302–14 (2002)
27. Drummond, C., Israelachvili, J.N.: Dynamic behavior of confined branched hydrocarbon lubricant fluids under shear. Macromolecules **33**(13), 4910–4920 (2000). doi:10.1021/ma9919918
28. Bouhacina, T., Aime, J.P., Gauthier, S., Michel, D.: Tribological behaviour of a polymer grafted on silanized silica probed with a nanotip. Phys. Rev. B **56**(12), 7694–7703 (1997). doi:10.1103/PhysRevB.56.7694
29. Johnson, K.L., Kendall, K., Roberts, A.D.: Surface energy and the contact of elastic solids. Proc. R. Soc. Lond. A Math. Phys. Sci. **324**, 301–313 (1971). doi:10.1098/rspa.1971.0141
30. Devaprakasam, D., Khatri, O.P., Shankar, N., Biswas, S.K.: Boundary lubrication additives for aluminium: a journey from nano to macrotribology. Trib. Int. **38**, 1022–1034 (2005). doi:10.1016/j.triboint.2005.07.030
31. He, G., Muser, M.H., Robbins, M.O.: Adsorbed layers and the origin of static friction. Science **284**, 1650–1652 (1999). doi:10.1126/science.284.5420.1650
32. DePalma, V., Tillman, N.: Friction and wear of self-assembled trichlorosilane monolayer films on silicon. Langmuir **5**, 868–872 (1989). doi:10.1021/la00087a049

33. Glosli, J.N., McClelland, G.M.: Molecular dynamics study of sliding friction or ordered organic monolayers. Phys. Rev. Lett. **70**(13), 1960–1963 (1993). doi:10.1103/PhysRevLett.70.1960
34. Gnecco, E., Bennewitz, R., Gyalog, T., Loppacher, C., Bammerlin, M., Meyer, E., et al.: Velocity dependence of atomic friction. Phys. Rev. Lett. **84**(6), 1172–1175 (2000). doi:10.1103/PhysRevLett.84.1172
35. Sang, Y., Dube, M., Grant, M.: Thermal effects of atomic friction. Phys. Rev. Lett. **87**(17), 174301-1-4 (2001)
36. Schirmeisen, A., Jansen, L., Fuchs, H.: Tip-jump statistics of stick-slip friction. Phys. Rev. B. **71**, 245403-1-7 (2005)
37. Zhang, Q., Archer, L.A.: Boundary lubrication and surface mobility of mixed alkylsilane self-assembled monolayers. J. Phys. Chem. B **107**, 13123–13132 (2003). doi:10.1021/jp035592x
38. Mikulski, P.T., Herman, L.A., Harrison, J.A.: Odd and even model self-assembled monolayers: links between friction and structure. Langmuir **21**, 12197–12206 (2005). doi:10.1021/la052044x
39. Mikulski, P.T., Harrison, J.A.: Periodicities in the properties associated with the friction of model self-assembled monolayers. Tribol. Lett. **10**(1–2), 29–35 (2001). doi:10.1023/A:1009066026845
40. Mikulski, P.T., Harrison, J.A.: Packing density effects on the friction of n-alkane monolayers. J. Am. Chem. Soc. **123**, 6873–6881 (2001). doi:10.1021/ja010189u
41. Mikulski, P.T., Gao, G., Chateauneuf, G.M., Harrison, J.A.: Contact forces at the sliding interface: mixed versus pure model alkane monolayers. J. Chem. Phys. **122**, 024701-1-9 (2005)
42. Chandross, M., Lorenz, C.D., Stevens, M.J., Grest, G.S.: Simulations of nanotribology with realistic probe tip models. Langmuir **24**, 1240–1246 (2008). doi:10.1021/la702323y
43. Tutein, A.B., Stuart, S.J., Harrison, J.A.: Indentation analysis of linear-chain hydrocarbon monolayers anchored to diamond. J. Phys. Chem. B **103**, 11357–11365 (1999). doi:10.1021/jp992687j
44. Harrison, J.A., Mikulski, P.T., Stuart, S.J., Tutein, A.B.: Dependence of frictional properties of hydrocarbon chains on tip contact area. In: Stephen, H.M., Charles, Y.Z. (eds.) Nanotribology, Critical Assessment and Research Needs. Kluwer Academic Publishers, Norwell (2002)
45. Salmeron, M.: Generation of defects in model lubricant monolayers and their contribution to energy dissipation in friction. Tribol. Lett. **10**(1–2), 69–79 (2001). doi:10.1023/A:1009026312732
46. Prathima, N., Harini, M., Rai, N., Chandrashekara, R.H., Ayappa, K.G., Sampath, S., Biswas, S.K.: Thermal study of accumulation of conformational disorders in the self assembled monolayers of C_8 and C_{18} alkanethiols on the Au (111) surface. Langmuir **21**, 2364–2374 (2005). doi:10.1021/la048654z
47. Bensebba, F., Ellis, T.H., Badia, A., Lennox, R.B.: Thermal treatment of n-alkanethiolate monolayers on gold, as observed by infrared spectroscopy. Langmuir **14**, 2361–2367 (1998). doi:10.1021/la9711589
48. Carpick, R.W., Salmeron, M.: Scratching the surface: fundamental investigations of tribology with atomic force microscopy. Chem. Rev. **97**, 1163–1194 (1997). doi:10.1021/cr960068q
49. Meyer, E., Overney, R.L., Brodbeck, D., Howald, L., Frommer, J., Guntherodt, H.-J., et al.: Friction force microscopy of mixed Langmuir-Blodgett films. Thin Solid Films **220**, 132–137 (1992). doi:10.1016/0040-6090(92)90561-O
50. Eaton, D.F., Smart, B.E.: Are fluorocarbon chains "stiffer" than hydrocarbon chains? Dynamics of end-to-end cyclization in a C_8F_{16} monitored by flurodcence. J. Am. Chem. Soc. **112**, 2821–2823 (1990). doi:10.1021/ja00163a065
51. Devaprakasam, D., Biswas, S.K.: Molecular damping: mechanical response of self-assembled monomolecular layer to compression. Phys. Rev. B **72**, 125434-1-8 (2005)
52. Shafrin, E.G., Zisman, W.A.: The adsorption on platinum and wettability of monolayers of terminally fluorinated octadecyl derivatives. J. Phys. Chem. **61**, 1046–1053 (1957). doi:10.1021/j150554a004
53. Israelachvili, J.N.: Intermolecular and Surface Forces, 2nd edn, ch. 4. Academic Press, New York (1992)
54. Alves, C.A., Porter, M.D.: Atomic force microscopic characterization of a fluorinated alkanethiolate monolayer at gold and correlations to electrochemical and infrared reflection spectroscopic structural descriptions. Langmuir **9**, 3507–3512 (1993). doi:10.1021/la00036a027